Inorg. Chem. **2000,** *39,* 2087−2095

Crystal Structures and Magnetic Properties of Metal Complexes Bearing Four Nitronyl Nitroxide Moieties in the Same Coordination Sphere

Giancarlo Francese,[†] Francisco M. Romero,*[,†,#] Antonia Neels,[‡] Helen Stoeckli-Evans,[‡] and Silvio Decurtins[†]

Departement für Chemie und Biochemie, Universität Bern, Freiestrasse 3,
CH-3012 Bern, Switzerland, and Institut de Chimie, Université de Neuchâtel,
Avenue de Bellevaux 51, CH-2000 Neuchâtel, Switzerland

Received October 21, 1999

Mononuclear transition metal complexes of the type $[M(2,6\text{-NITpy})_2](ClO_4)_2 \times$ solvent (2,6-NITpy = 2,6-bis-(3′-oxide-1′-oxyl-4′,4′,5′,5′-tetramethylimidazolin-2′-yl)pyridine; M = Ni (**1**), Co (**2**), Zn (**3**), Mn (**4**), Cu (**5**)) have been synthesized and characterized by single-crystal X-ray diffraction studies. Crystal data: **1**, monoclinic, $P2_1/c$, $Z = 4$, $a = 20.946(2)$ Å, $b = 12.0633(2)$ Å, $c = 21.173(2)$ Å, $\beta = 113.55(1)°$; **2**, monoclinic, $P2_1/c$, $Z = 4$, $a = 20.902(2)$ Å, $b = 12.0981(8)$ Å, $c = 21.215(2)$ Å, $\beta = 113.130(9)°$; **3**, triclinic, $P\bar{1}$, $Z = 2$, $a = 11.410(1)$ Å, $b = 12.932(1)$ Å, $c = 21.609(2)$ Å, $\alpha = 96.040(2)°$, $\beta = 102.24(1)°$, $\gamma = 114.98(1)$; **4**, monoclinic, $P2_1/n$, $Z = 4$, $a = 11.5473(8)$ Å, $b = 19.212(1)$ Å, $c = 25.236(2)$ Å, $\beta = 98.772(9)°$; **5**, triclinic, $P\bar{1}$, $Z = 2$, $a = 12.1604(9)$ Å, $b = 12.6961(9)$ Å, $c = 18.103(2)$ Å, $\alpha = 84.191(8)°$, $\beta = 73.392(8)°$, $\gamma = 66.072(8)$. The two 2,6-NITpy biradicals behave as terdentate ligands and bind almost perpendicular to each other in meridional positions. In compounds **1**−**4**, the pyridine rings are axially ligated and four different nitronyl nitroxide radicals bind to the metal center through their O(nitroxyl) atoms, forming the equatorial plane of a distorted octahedron. On the contrary, in the copper(II) complex (**5**), the two N(pyridyl) atoms are found in equatorial positions. Only two nitroxide groups are then bound to the copper(II) ion in the equatorial plane, the other two being axially ligated. The two axially bound nitronyl nitroxide radicals couple ferromagnetically to the copper center ($J_{Cu-rad(ax)} = +10$ K), whereas a strong antiferromagnetic coupling between this metal ion and the equatorial nitroxide groups ($J_{Cu-rad(eq)} = -460$ K) is observed. The other complexes exhibit strong antiferromagnetic metal−radical interactions: $J_{Ni-rad} = -240$ K, for **1**; $J_{Mn-rad} = -120$ K, for **4**. Interestingly, the study of the diamagnetic zinc(II) compound (**3**) reveals a moderate intramolecular antiferromagnetic interaction between radicals coordinated to the same metal center ($J_{rad-rad} = -27.7$ K). This interaction is transmitted through space and is also present in the other complexes: $J_{rad-rad} = -14$ K, for **1**; $J_{rad-rad} = -10$ K, for **4**; $J_{rad-rad} = -20.5$ K, for **5**. Antiferromagnetic intermolecular interactions are also present in all the complexes herein studied.

Introduction

The synthesis and study of transition metal compounds incorporating organic free radicals directly bound to their coordination sphere[1,2] is a major research aim in the field of molecular magnetism.[3,4] A great advantage is taken from the fact that exchange interactions result from direct overlap between metal and radical magnetic orbitals. These interactions are then generally strong and can be easily correlated to structural factors.

Nitroxide free radicals are normally used as organic spin carriers due to their exceptional stability and ease of chemical modification.[5] Among them, nitronyl nitroxide radicals became popular because of their ability to act as bridging ligands. However, the weakly basic character of these radicals makes coordination possible only if the metal center is activated with electron-withdrawing groups. Precursors of the type $M(hfac)_2$ (hfac = hexafluoroacetylacetonato) in which the electron-withdrawing ligands occupy four coordination sites are currently employed.[6] Only two vacant sites are available for ligation of the radical species, and this situation leads invariably to systems of restrained dimensionality. In most of the systems studied so far, the nitronyl nitroxides act in a bridging mode and are found in axial positions, thus leading to metal−radical alternating chains that may order ferromagnetically only at low temperatures.[7,8]

To overcome these limitations, two basic strategies have been developed. One approach uses high-spin *tert*-butylnitroxide polyradicals as bridging units between the $M(hfac)_2$ entities. Two- and three-dimensional structures with fascinating magnetic

---

[†] Universität Bern.

[‡] Université de Neuchâtel.

[#] Present address: Universitat de València, Departament de Química Inorgànica, Dr. Moliner, 50, E-46100-Burjassot (València), Spain. E-mail: Fco.Manuel.Romero@uv.es.

(1) Caneschi, A.; Gatteschi, D.; Sessoli, R.; Rey, P. *Acc. Chem. Res.* **1989**, *22*, 392−398.

(2) Caneschi, A.; Gatteschi, D.; Rey, P. *Prog. Inorg. Chem.* **1991**, *39*, 331−429.

(3) Coronado, E., Delhaès, P., Gatteschi, D., Miller, J. S., Eds. *Molecular Magnetism: From Molecular Assemblies to the Devices*; NATO ASI Series E321; Kluwer Academic Publishers: Dordrecht, 1996.

(4) Kahn, O. *Molecular Magnetism*; VCH: New York, 1993.

(5) Volodarsky, L. B.; Reznikov, V. A.; Ovcharenko, V. I. *Synthetic Chemistry of Stable Nitroxides*; CRC Press: London, 1994.

(6) Caneschi, A.; Ferraro, F.; Gatteschi, D.; Rey, P.; Sessoli, R. *Inorg. Chem.* **1990**, *29*, 1756−1760.

(7) Caneschi, A.; Gatteschi, D.; Laugier, J.; Rey, P. *J. Am. Chem. Soc.* **1987**, *109*, 2191−2192.

(8) Luneau, D.; Rey, P.; Laugier, J.; Fries, P.; Caneschi, A.; Gatteschi, D.; Sessoli, R. *J. Am. Chem. Soc.* **1991**, *113*, 1245−1251.

10.1021/ic991236a CCC: $19.00

properties can be obtained in this way by using polyradicals possessing three or more nitroxide donors.[9−11] In the second approach a nitronyl nitroxide moiety is incorporated into a ligand in such a way that complexation to simple metal salts proceeds via the chelate effect. Along this line, pyridine,[12] 2,2′-bipyridine,[13−16] and triazole[17,18] units have been functionalized to give suitable ligands for metal complexation. Amines bearing pendant nitronyl nitroxide groups have also been synthesized[19,20] and used in the EPR detection of alkaline ions.[19] Recently, nitroxide ligands based on imidazole subunits have been successfully employed in the construction of extended structures.[21,22] A two-dimensional compound ordering at 40 K has been reported.[23]

An interesting point is that this second strategy offers the oportunity to tune the radical−metal interactions giving rise to special magnetic properties. For example, metal−radical ferromagnetic interactions can be induced by an appropriate ligand design.[15,16] Pseudo spin transitions can even be observed due to small variations of geometrical parameters.[24,25] Systems showing spin frustration have also been studied.[26] All these examples show that the study of the magnetism of these systems is particularly rich and deserves more attention.

In most of the cases studied so far, only two nitroxide radicals are bound to the metal through the nitroxyl oxygen atom. We report herein on the synthesis of 1:2 metal complexes of the ligand 2,6-NITpy (2,6-NITpy = 2,6-bis(3′-oxide-1′-oxyl-4′,4′,5′,5′-tetramethylimidazolin-2′-yl)pyridine). This terdentate biradical affords compounds having four nitroxide ligands directly bound to the metal center. A study of the magnetic properties of compounds of the type $[M(2,6\text{-NITpy})_2](ClO_4)_2$ (M = Mn, Co, Ni, Cu, Zn) has been performed. Structural characterization is provided for all the metal complexes herein described.

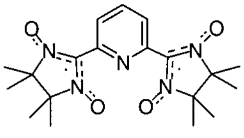

2,6-NITpy

Experimental Section

(A) Materials. 2,3-Bis(hydroxylamino)-2,3-dimethylbutane,[29] 2,6-pyridinedicarboxaldehyde,[30] and 2,6-NITpy[13] were prepared using adapted literature procedures. Perchlorate salts were used as purchased.

CAUTION: *Note that perchlorate salts should be handled carefully, in low quantities, used as hydrated salts, and never dehydrated under vacuum before use.*

(a) Preparation of Complexes 1 and 2. Stoichiometric amounts of 2,6-NITpy (100 mg scale) and $M(ClO_4)_2{\cdot}6H_2O$ (M = Ni, Co) were mixed in 15 mL of methanol. The resultant brown solution was filtered over Celite and evaporated slowly. After a few days of standing, platelike crystals were isolated.

(b) Preparation of Complexes 3 and 5. Stoichiometric amounts of 2,6-NITpy (100 mg scale) in dichloromethane (10 mL) and $M(ClO_4)_2{\cdot}6H_2O$ (M = Zn, Cu) in ethyl acetate (10 mL) were mixed, affording a fast color change from blue to black (in the case of zinc) and brown (in the case of copper). Stirring the solution for 20 min led to quantitative precipitation of the complexes, which were recovered by centrifugation and washed with ethyl acetate and diethyl ether. Recrystallization from an acetonitrile/toluene (ca. 1/1) solution gave well-formed single crystals of the desired complex. Elemental analysis was performed on dry powdered samples.

(c) Preparation of Complex 4. Diluted solutions of 2,6-NITpy (100 mg scale) in dichloromethane (75 mL) and $Mn(ClO_4)_2{\cdot}6H_2O$ (0.5 equiv) in ethyl acetate (75 mL) were mixed, affording a fast color change from blue to green as a consequence of complexation. The resultant green solution was filtered over a Celite pad and evaporated slowly. After a few days of standing, platelike crystals were isolated. The crystals contain ethyl propionate, which is present in the solvent as an impurity. Elemental analysis was performed on dry powdered samples.

$[Ni(2,6\text{-NITpy})_2](ClO_4)_2{\cdot}0.5H_2O{\cdot}0.5CH_3OH$ (1): 72%; ES-MS (CH_3CN) 938.3 $[M - ClO_4]^+$, 422.67 $[M - 2ClO_4]^{2+}$; IR (KBr pellet, cm^{-1}) 1591 (m), 1465 (m), 1340 (s) (ν_{NO}), 1147 (m), 1095 (m) (ν_{ClO}), 817 (s), 625 (m); UV (CH_3CN) λ (nm) (ϵ ($M^{-1}\ cm^{-1}$)) 569 (2800), 408 (14 100), 367 (24 700), 328 (22 000), 266 (30 000), 237 (36 000). Anal. Calcd for $C_{38}H_{54}N_{10}O_{16}NiCl_2{\cdot}0.5H_2O{\cdot}0.5CH_3OH$ ($M_r = 1\,036\,517 + 9007 + 16\,021$): C, 43.23; H, 5.30; N, 12.93. Found: C, 43.11; H, 5.57; N, 12.89.

$[Co(2,6\text{-NITpy})_2](ClO_4)_2{\cdot}0.5H_2O{\cdot}CH_3OH$ (2): 75%; ES-MS (CH_3CN) 938.3 $[M - ClO_4]^+$, 419.4 $[M - 2ClO_4]^{2+}$; IR (KBr pellet, cm^{-1}) 1591 (m), 1459 (m), 1340 (s) (ν_{NO}), 1168 (m), 1095 (m) (ν_{ClO}), 817 (s), 632 (m); UV (CH_3CN) λ (nm) (ϵ ($M^{-1}\ cm^{-1}$)) 563 (1700), 369 (20 000), 268 (25 000), 239 (27 000). Anal. Calcd for $C_{38}H_{54}N_{10}O_{16}CoCl_2{\cdot}0.5H_2O{\cdot}CH_3OH$ ($M_r = 1\,036\,750 + 9007 + 32\,042$): C, 43.14; H, 5.48; N, 12.90. Found: C, 42.95; H, 5.36; N, 13.0.

$[Zn(2,6\text{-NITpy})_2](ClO_4)_2{\cdot}2.5CH_3CN$ (3): 91%; ES-MS (CH_3CN) 944.79 $[M - ClO_4]^+$, 422.66 $[M - 2ClO_4]^{2+}$; IR (KBr pellet, cm^{-1}) 1591 (m), 1465 (m), 1340 (s) (ν_{NO}), 1147 (m), 1095 (m) (ν_{ClO}), 817 (s), 625 (m); UV (CH_3CN) λ (nm) (ϵ ($M^{-1}\ cm^{-1}$)) 564 (1700), 369 (29 000), 320 (21 000), 266 (26 000), 239 (27 000). Anal. Calcd for $C_{38}H_{54}N_{10}O_{16}ZnCl_2$ ($M_r = 1\,043\,197$): C, 43.75; H, 4.22; N, 13.43. Found: C, 43.47; H, 4.21; N, 13.43.

$[Mn(2,6\text{-NITpy})_2](ClO_4)_2{\cdot}1.5CH_2Cl_2{\cdot}0.5C_5H_{10}O_2$ (4): 85%; ES-MS (CH_3CN) 934.30 $[M - ClO_4]^+$, 417.43 $[M - 2ClO_4]^{2+}$; IR (KBr pellet, cm^{-1}) 1588 (m), 1459 (m), 1338 (s) (ν_{NO}), 1136 (m), 1091 (m) (ν_{ClO}), 812 (s), 621 (m); UV (CH_3CN) λ (nm) (ϵ ($M^{-1}\ cm^{-1}$)) 560 (2100), 372 (25 000), 330 (24 000), 261 (28 000), 239 (31 000). Anal. Calcd

---

(9) Inoue, K.; Iwamura, H. *J. Am. Chem. Soc.* **1994**, *116*, 3173−3174.
(10) Inoue, K.; Iwamura, H. *Adv. Mater.* **1996**, *8*, 73−75.
(11) Inoue, K.; Hayamizu, T.; Iwamura, H.; Hashizume, D.; Ohashi, Y. *J. Am. Chem. Soc.* **1996**, *118*, 1803−1804.
(12) Luneau, D.; Risoan, G.; Rey, P.; Grand, A.; Caneschi, A.; Gatteschi, D.; Laugier, J. *Inorg. Chem.* **1993**, *32*, 5616−5622.
(13) Ulrich, G.; Ziessel, R.; Luneau, D.; Rey, P. *Tetrahedron Lett.* **1994**, *35*, 1211−1214.
(14) Luneau, D.; Laugier, J.; Rey, P.; Ulrich, G.; Ziessel, R.; Legoll, P.; Drillon, M. *J. Chem. Soc., Chem. Commun.* **1994**, 741−742.
(15) Romero, F. M.; Luneau, D.; Ziessel, R. *J. Chem. Soc., Chem. Commun.* **1998**, 551−552.
(16) Luneau, D.; Romero, F. M.; Ziessel, R. *Inorg. Chem.* **1998**, *37*, 5078−5087.
(17) Pei, Y.; Lang, A.; Bergerat, P.; Kahn, O.; Fettouhi, M.; Ouahab, L. *Inorg. Chem.* **1996**, *35*, 193−198.
(18) Sutter, J.-P.: Kahn, M. L.; Golhen, S.; Ouahab, L.; Kahn, O. *Chem. Eur. J.* **1998**, *4*, 571−576.
(19) Ulrich, G.; Turek, P.; Ziessel, R.; De Cian, A.; Fischer, J. *J. Chem. Soc., Chem. Commun.* **1996**, 2461−2462.
(20) Vostrikova, K. E.; Belorizky, E.; Pécaut, J.; Rey, P. *Eur. J. Inorg. Chem.* **1999**, 1181−1187.
(21) Fegy, K.; Sanz, N.; Luneau, D.; Belorizky, E.; Rey, P. *Inorg. Chem.* **1998**, *37*, 4518−4523.
(22) Fegy, K.; Luneau, D.; Belorizky, E.; Novac, M.; Tholence, J.-L.; Paulsen, C.; Ohm, T.; Rey, P. *Inorg. Chem.* **1998**, *37*, 4524−4532.
(23) Fegy, K.; Luneau, D.; Ohm, T.; Paulsen, C.; Rey, P. *Angew. Chem., Int. Ed. Engl.* **1998**, *37*, 1270−1273.
(24) Lanfranc de Panthou, F.; Belorizky, E.; Calemczuk, R.; Luneau, D.; Marcenat, C.; Ressouche, E.; Turek, P.; Rey, P. *J. Am. Chem. Soc.* **1995**, *117*, 11247−11253.
(25) Lanfranc de Panthou, F.; Luneau, D.; Musin, R.; Öhrström, L.; Grand, A.; Turek, P.; Rey, P. *Inorg. Chem.* **1996**, *35*, 3484−3491.
(26) Tanaka, M.; Matsuda, K.; Itoh, T.; Iwamura, H. *Angew. Chem., Int. Ed. Engl.* **1998**, *37*, 810−812.
(27) Sheldrick, G. M. *Acta Crystallogr.* **1990**, *A46*, 467−473.
(28) Sheldrick, G. M. *SHELXL-97, Program for crystal structure refinement*; University of Göttingen: Germany, 1997.
(29) Lamchen, M.; Mittag, T. W. *J. Chem. Soc. C* **1966**, 2300−2303.
(30) Papadopoulos, E. P.; Jarrar, A.; Issidorides, C. H. *J. Am. Chem. Soc.* **1966**, *31*, 615−616.

Table 1. Summary of the Crystal Structure Data Collection and Refinement for **1**−**5**

	1	**2**	**3**	**4**	**5**
chemical formula	$C_{38}H_{54}N_{10}O_{16}Cl_2Ni\cdot 0.5CH_3OH\cdot 0.5H_2O$	$C_{38}H_{54}N_{10}O_{16}Cl_2Co\cdot CH_3OH\cdot 0.5H_2O$	$C_{38}H_{54}N_{10}O_{16}Cl_2Zn\cdot 2.5CH_3CN$	$C_{38}H_{54}N_{10}O_{16}Cl_2Mn\cdot 1.5CH_2Cl_2\cdot 0.5C_5H_{10}O_2$	$C_{38}H_{54}N_{10}O_{16}Cl_2Cu\cdot CH_3CN$
fw	1060.54	1076.78	1145.82	1211.21	1082.41
T (°C)	−50(3)	−50(2)	−50(2)	−50(2)	−70(2)
space group	$P2_1/c$ (No. 14)	$P2_1/c$ (No. 14)	$P\bar{1}$ (No. 2)	$P2_1/n$ (No. 14)	$P\bar{1}$ (No. 2)
Z	4	4	2	4	2
a (Å)	20.946(2)	20.902(2)	11.410(1)	11.5473(8)	12.1604(9)
b (Å)	12.0633(2)	12.0981(8)	12.932(1)	19.212(1)	12.6961(9)
c (Å)	21.173(2)	21.215(2)	21.609(2)	25.236(2)	18.103(2)
α (deg)	90	90	96.040(2)	90	84.191(8)
β (deg)	113.55(1)	113.130(9)	102.24(1)	98.772(9)	73.392(8)
γ (deg)	90	90	114.98(1)	90	66.072(8)
V (Å^3)	4904.1(7)	4937.7(7)	2755.1(5)	5533.1(6)	2447.8(3)
ρ_{calcd} (g cm^{-3})	1.436	1.448	1.381	1.454	1.469
μ(Mo Kα) (cm^{-1})	5.83	5.36	6.18	5.55	6.35
λ (Å)	0.71073	0.71073	0.71073	0.71073	0.71073
$R(F_o)^a$, $I > 2\sigma(I)$	0.0535	0.0467	0.0645	0.0573	0.0396
$R_w(F_o)^b$, $I > 2\sigma(I)$	0.1111	0.0891	0.1690	0.1721	0.0571

[a] $R(F_o) = \sum(|F_o| - |F_c|)/\sum|F_o|$. [b] $R_w(F_o) = \sum(w|F_o|^2 - |F_c|^2/\sum w|F_o|^4)^{1/2}$.

for $C_{38}H_{54}N_{10}O_{16}MnCl_2$ (M_r = 1 043 197): C, 44.19; H, 5.27; N, 13.56. Found: C, 44.47; H, 5.25; N, 13.18.

[Cu(2,6-NITpy)$_2$](ClO$_4$)$_2$·CH$_3$CN (5): 85%; ES-MS (CH$_3$CN) 942.80 [M − ClO$_4$]$^+$, 421.67 [M − 2ClO$_4$]$^{2+}$; IR (KBr pellet, cm^{-1}) 1591 (m), 1465 (m), 1340 (s) (ν_{NO}), 1147 (m), 1095 (m) (ν_{ClO}), 817 (s), 625 (m); UV (CH$_3$CN) λ (nm) (ϵ (M^{-1} cm^{-1})) 564 (1700), 369 (29 000), 320 (21 000), 266 (26 000), 239 (27 000). Anal. Calcd for $C_{38}H_{54}N_{10}O_{16}CuCl_2$ (M_r = 1041 363): C, 43.83; H, 5.23; N, 13.45. Found: C, 43.65; H, 5.44; N, 13.77.

(B) X-ray Crystal Structure Analysis. Single crystals of compounds **1**−**5** were mounted on a Stoe imaging plate diffractometer system (Stoe & Cie, 1995) equipped with a one-circle φ goniometer and a graphite-monochromator. Data collection was performed at −50 °C using Mo Kα radiation (λ = 0.710 73 Å); 195 exposures (3 min per exposure) were obtained at an image plate distance of 70 mm with 0° < φ < 195° and with the crystal oscillating through 1° in φ. The resolution was $D_{min} - D_{max}$ = 12.45−0.81 Å.

The structures were solved by direct methods using the program SHELXS-97[27] and refined by full-matrix least-squares on F^2 with SHELXL-97.[28] The hydrogen atoms were included in calculated positions and treated as riding atoms using SHELXL-97 default parameters. No absorption corrections were applied. The R_{int} values for **1** and **2** are large (>0.10) probably due to the poor quality of the crystals, which exhibited a large mosaic spread, rather than due to absorption effects. One disordered molecule of methanol (having an occupancy factor of 0.5 for **1**) and one water molecule, the latter having an occupancy of 0.5, were found per asymmetric unit in the molecular structures of **1** and **2.** Two molecules of acetonitrile with occupancies of 1.0, one being disordered and one acetonitrile having an occupancy of 0.5, were found per asymmetric unit in the molecular structure of **3**. A disorder was also found in one ligand molecule with occupancies of 0.5 for atoms C9, C10, C11, C12, C9A, C10A, C11A, and C12A, and both perchlorate anions were found to be strongly disordered, too. Two molecules of dichloromethane, one of them having an occupancy of 0.5, and one molecule of ethyl propionate having also an occupancy of 0.5 were found per asymmetric unit in the molecular structure of **4**. One of two perchlorate anions was found to be disordered, having occupancies of 0.5 for all chlorine atoms, and one molecule of acetonitrile was found per asymmetric unit in the molecular structure of **5**. All non-hydrogen atoms were refined anisotropically. Crystal structure and refinement data are summarized in Table 1 for compounds **1**−**5**.

(C) Magnetic Susceptibility Measurements. The magnetic susceptibility was measured on polycrystalline samples in the 1.8−300 K temperature range for each compound with a Quantum Design MPMS superconducting SQUID magnetometer operating at a field strength of 1 kOe. The data were corrected for diamagnetism of the constituent atoms using Pascal constants.

Results

Structural Studies. The crystal structures of complexes **1**−**5** show that biradical 2,6-NITpy behaves as a terdentate ligand with the N(pyridyl) atom and the two O(nitroxyl) atoms occupying meridional positions of a distorted octahedron. The metal center is surrounded by two 2,6-NITpy ligands that are arranged almost perpendicular to one another. The conformation of the biradical chelate is similar to that found in other free aryl-substituted nitronyl nitroxides. The torsion angles between the pyridyl rings and the radical moieties lie, unless otherwise specified, in a range between 26° and 34°. A detailed analysis of the geometrical parameters that may be correlated to the magnetic properties of the complexes has been performed. These are mainly intramolecular dihedral angles between planes located parallel or perpendicular to the directions of the magnetic orbitals. The values are gathered in Table 2.

[M(2,6-NITpy)$_2$](ClO$_4$)$_2$·0.5H$_2$O·*m*CH$_3$OH [M = Ni (1), Co (2)]. Compounds **1** and **2** are isostructural and crystallize in the centrosymmetric space group $P2_1/c$. Both crystals are solvates and contain one water molecule showing half occupancy. Compound **2** crystallizes with one molecule of methanol, whereas in compound **1** this molecule has an occupancy factor of 1/2. A view of the Ni(II) cationic complex is shown in Figure 1. The equatorial plane is formed by four oxygen atoms belonging to the free radicals. Within this plane there is no significant distortion: the Ni−O bond lengths have similar values, ranging from 2.021(3) Å (Ni−O7) to 2.037(3) Å (Ni−O1), and the O−Ni−O angles are close to 90°. The two axial positions are occupied by two N(pyridyl) atoms at 2.065 ± 0.005 Å. The N1−Ni−O5 angle (95.27(13)°) shows the largest deviation from the value of 90° expected for an ideal octahedron.

The isostructural cobalt(II) compound **2** has a very similar structure. The Co−O distances in the equatorial plane are slightly larger, going from 2.034(3) Å (Co−O3) to 2.062(2) Å (Co−O5). Two pyridyl N atoms occupy the axial positions at 2.115 ± 0.004 Å. The N1−Co−O5 angle shows again the largest deviation (96.78(13)°) from the ideal value.

Particularly interesting is the proximity between adjacent radical subunits within the complexes. For both compounds, other than the O−O contacts in the equatorial plane, there are nine interatomic contacts between radicals below 3 Å, with the shortest distance (O7−N4) equal to 2.767(3) Å (for **1**) and 2.796(3) Å (for **2**). The shortest intermolecular contact between

Table 2. Selected Intramolecular Dihedral Angles

Least-squares mean planes have been defined as follows (see Figures 1 and 3):

equatorial plane ($x^2 - y^2$):	O1−O3−O5−O7	rad 1: O1−N2−C6−N3−O2	rad 2: O5−N7−C25−N8−O6
xz plane:	O1−N1−O3−N6	rad 3: O3−N4−C13−N5−O4	rad 4: O7−N9−C32−N10−O8
yz plane:	O5−N1−O7−N6		

dihedral angle	**1**(Ni)	**2**(Co)	**3**(Zn)	**4**(Mn)	**5**(Cu)[a]
equatorial plane, rad1	67.24(08)°	66.89(07)°		54.72(17)°	51.83(22)°
equatorial plane, rad2	64.21(21)°	65.03(17)°		59.03(19)°	50.39(19)°
equatorial plane, rad3	60.02(34)°	59.53(28)°		75.76(15)°	55.73(14)°
equatorial plane, rad4	65.79(32)°	64.90(26)°		64.89(18)°	43.43(33)°
xz plane, rad1	54.60(19)°	55.48(16)°		58.65(23)°	
xz plane, rad2	47.96(36)°	47.80(30)°		41.62(21)°	
xz plane, rad3	56.08(26)°	56.16(21)°		54.69(17)°	
xz plane, rad4	48.08(25)°	47.95(20)°		48.61(17)°	
yz plane, rad1	44.27(40)°	43.63(33)°		49.33(17)°	
yz plane, rad2	53.88(15)°	53.53(13)°		60.90(14)°	
yz plane, rad3	48.11(38)°	49.61(31)°		39.71(23)°	
yz plane, rad4	51.05(17)°	51.61(13)°		55.22(20)°	
rad1, rad2	81.85(35)°	82.85(25)°	81.21(46)°	71.29(25)°	60.37(24)°
rad1, rad3	52.72(40)°	53.58(33)°	54.48(27)°	49.56(26)°	52.24(30)°
rad1, rad4	77.38(39)°	76.68(31)°	77.14(32)°	72.74(25)°	84.74(29)°
rad2, rad3	75.97(44)°	76.05(37)°	83.78(38)°	86.18(27)°	80.12(27)°
rad2, rad4	50.05(30)°	50.09(25)°	52.94(51)°	56.36(21)°	67.48(27)°
rad3, rad4	81.46(39)°	80.41(31)°	81.77(39)°	85.60(25)°	80.22(27)°

[a] Equatorial plane for **5**(Cu) is O1−N1−O3−N6.

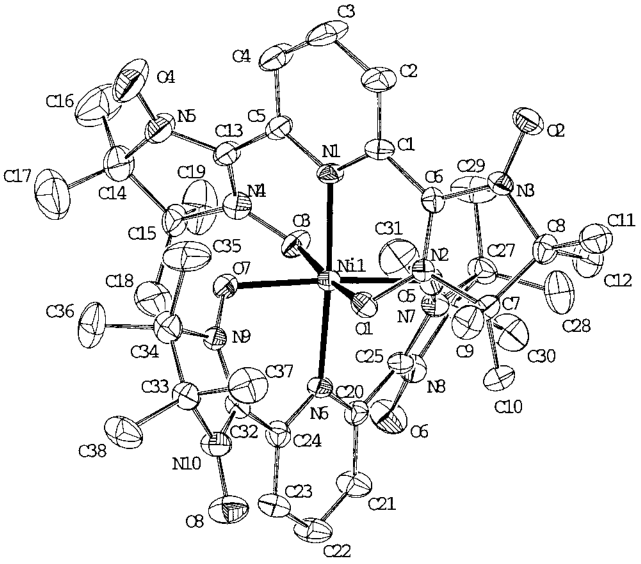

Figure 1. ORTEP[42] view of the $[Ni(2,6\text{-}NITpy)_2]^{2+}$ cation in complex **1**, showing the numbering of the atoms.

uncoordinating N−O groups corresponds to O6−O2(*x*, 3/2−*y*, *z*−1/2): 3.307(3) Å (for **1**) and 3.272(3) Å (for **2**).

$[Zn(2,6\text{-}NITpy)_2](ClO_4)_2 \cdot 2.5CH_3CN$ (3). The zinc(II) complex crystallizes in the triclinic space group $P\bar{1}$ but has structural features similar to that of the nickel(II) and cobalt(II) compounds. The Zn−O distances are larger, ranging from 2.063(3) Å (Zn−O5) to 2.082(3) Å (Zn−O3). The two N(pyridyl) atoms, N1 and N6, are located at 2.136(3) and 2.146(3) Å, respectively. Slight deviations from the octahedral geometry are found in the equatorial plane (O3−Zn−O5 angle: 93.33(13)°) and out of this plane (N1−Zn−O7 angle: 95.89(13)°). There are seven contacts between adjacent radicals below 3 Å, and the shortest distance is O7−N2: 2.851(3) Å. The shortest intermolecular distance between uncoordinating N−O groups corresponds to O4−O8(*x*+1, *y*, *z*): 3.596(3) Å.

$[Mn(2,6\text{-}NITpy)_2](ClO_4)_2 \cdot 1.5CH_2Cl_2 \cdot 0.5C_5H_{10}O_2$ (4). This manganese(II) complex crystallizes in the monoclinic space group $P2_1/n$. The metal−ligand bond lengths are significantly longer than those found in complexes **1**−**3**. In the equatorial plane, the Mn−O5 distance (2.117(2) Å) is slightly longer than the other three Mn−O distances (average: 2.087(4) Å). The distances between the metal center and the two axial nitrogen atoms, N1 and N6, are 2.284(2) and 2.277(2) Å, respectively. The octahedral environment of the Mn(II) ion is severely distorted: the O3−Mn−O5 angle, in the equatorial plane, is 95.35(8)° and the N1−Mn−O7 angle is now equal to 110.50(9)°. There is a relationship between the degree of distortion and the size of the metal ion for all the complexes studied. As the size of the cation becomes large, the bond lengths in the coordination sphere increase and the ligands cannot wrap around the metal to occupy two opposite positions in the equatorial plane. For the Mn(II) compound, atoms O1 and O3 belonging to one ligand lie at an average distance of 0.332 ± 0.015 Å above the mean equatorial plane. The oxygen atoms corresponding to the other ligand, O5 and O7, are located below the plane at the same distance. For the other compounds the corresponding distances are as follows: **1**, 0.094(2) Å; **2**, 0.139(2) Å; **3**, 0.165 ± 0.006 Å. These effects are illustrated in Figure 2.

Five contacts shorter than 3 Å are found between proximate radicals in the coordination sphere, the shortest distance being 2.895(2) Å (O5−N2) . From an intermolecular point of view, the shortest distance between uncoordinating N−O functions is 3.565(2) Å (O4−O4(2−*x*, 1−*y*, 1−*z*)).

$[Cu(2,6\text{-}NITpy)_2](ClO_4)_2 \cdot CH_3CN$ (5). This compound crystallizes in the space group $P\bar{1}$. An ORTEP view of the cation is shown in Figure 3. The copper(II) ion is, as expected, in an elongated octahedral site (Jahn−Teller effect). The main difference with respect to compounds **1**−**4** is that the axial positions are now occupied by two O(nitroxyl) atoms of the same biradical instead of N(pyridyl) atoms. This was not unexpected since Cu−N(pyridyl) bonds are particularly stable due to metal-to-ligand charge transfer. Nitrogen donors bind then in equatorial positions, and the more distant axial positions are occupied by oxygen donors. In this complex, the Cu−N bond lengths are 2.019(3) Å (Cu−N1) and 2.036(3) Å (Cu−N6); the Cu−O bond distances in the equatorial plane are 1.955 ± 0.004 Å, whereas the two axial O(nitroxyl) atoms, O5 and O7, are located at

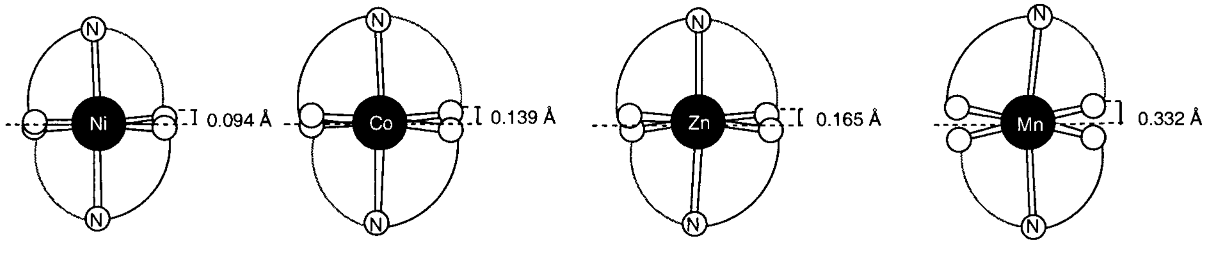

1 **2** **3** **4**

Figure 2. Comparison between the different metal environments found in compounds **1**−**4**. Note the correlation between the distortion of the coordination sphere and the size of the metal ion.

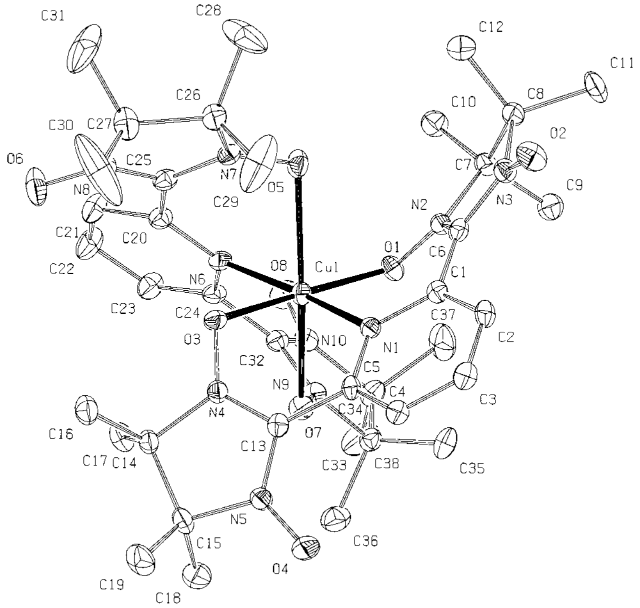

Figure 3. ORTEP view of the $[Cu(2,6\text{-NITpy})_2]^{2+}$ cation in complex **5**, showing the numbering of the atoms. Thermal ellipsoids are plotted at the 30% probability level.

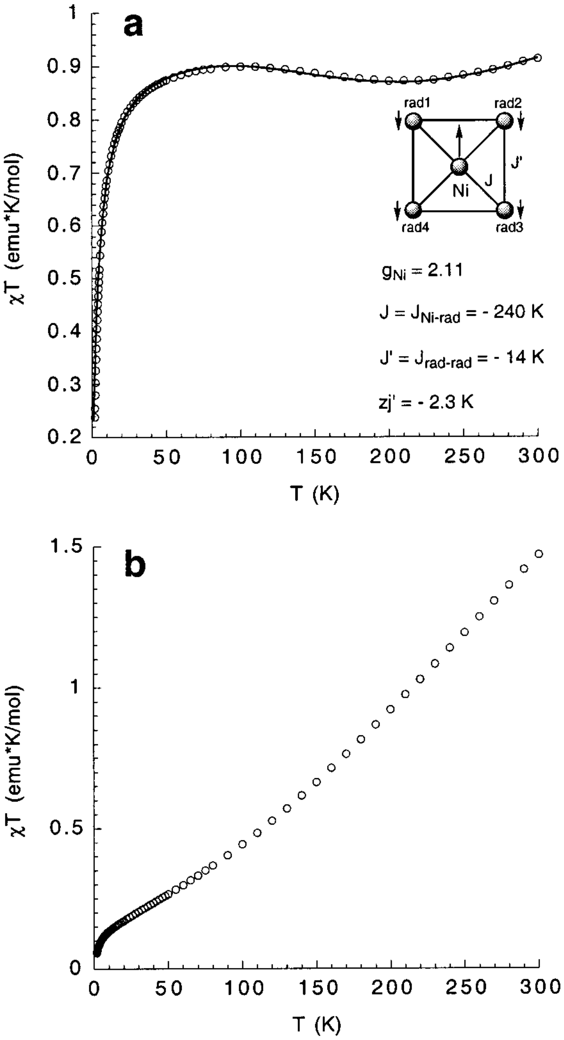

Figure 4. Temperature dependence of the product of the molar magnetic susceptibility with temperature (χT) for **1** (a) and **2** (b). The solid line represents the best-fit calculated data. Inset: Exchange interaction pattern and values of the calculated parameters.

2.337(3) and 2.255(3) Å, respectively. These are relatively low values for Cu(II)−O(axial) bond lengths. This effect is presumably due to the constraints imposed by the ligand. Inversely, the conformation of the biradical that occupies the axial positions is highly distorted. The torsion angle between the pyridine ring and one radical subunit (N6−C24−C32−N9) is 45.8(6)°. Here the equatorial plane is well defined by the atoms N1, O1, N6, and O3. Within this plane, the N6−Cu−O3 angle (98.58(12)°) shows a prominent deviation from the ideal value. Out of the equatorial plane, the more distorted bond angle corresponds to 81.50(12)° (N6−Cu−O5).

There are, within the same coordination sphere, eight interatomic contacts between radicals below 3 Å. The shortest distance is between an oxygen atom and an α-carbon atom of an adjacent radical (O3−C25: 2.724(3) Å). The molecular units are more isolated than in compounds **1**−**4**: the closest contact between uncoordinating N−O groups is 4.745(3) Å (O2−O8-(*x*+1, *y*, *z*)).

Magnetic Properties. The temperature dependence of the molar magnetic susceptibility χ has been measured in the 1.8−300 K range for complexes **1**−**5**. The results are displayed in the form of χT versus T plots, T being the absolute temperature.

$[Ni(2,6\text{-NITpy})_2](ClO_4)_2\cdot 0.5H_2O\cdot 0.5CH_3OH$ (1). At room temperature, the value of the χT product (0.91 emu K mol^{-1}) is much smaller (Figure 4a) than the expected high-temperature limit for a nickel(II) center ($g = 2.1$) and four nitroxide radicals ($\chi T = 2.60$ emu K mol^{-1}). As the temperature decreases, χT decreases and reaches a minimum at 200 K, where it has a value of 0.87 emu K mol^{-1}. Then χT increases and exhibits a nearly constant value (0.90 emu K mol^{-1}) in the 140−70 K temperature range, corresponding to a $S = 1$ ground state. At lower temperatures, the χT product drops steadily and equals 0.24 emu K mol^{-1} at 1.87 K.

This magnetic behavior is clearly indicative of antiferromagnetic interactions. For a system like compound **1**, a minimum in the χT versus T curve is expected. This minimum arises from a compensation between the short-range nickel−nitroxide antiferromagnetic coupling and the parallel alignment of the four $S = 1/2$ spins. The position of the minimum is highly dependent on the value of the metal−radical exchange coupling parameter, J_{Ni-rad}. Furthermore, strong antiferromagnetic coupling between the Ni(II) cation and the nitroxide radicals results in the $S = 1$ ground state observed at low temperatures. A quantitative description of the susceptibility data is possible by diagonalization of the isotropic Hamiltonian:

$$H = -2J_{Ni-rad}(S_{Ni}S_{rad1} + S_{Ni}S_{rad2} + S_{Ni}S_{rad3} + S_{Ni}S_{rad4}) - 2J_{rad-rad}(S_{rad1}S_{rad2} + S_{rad2}S_{rad3} + S_{rad3}S_{rad4} + S_{rad4}S_{rad1}) \quad (1)$$

where a radical−radical exchange coupling parameter, $J_{rad-rad}$, has also been considered (see zinc complex). Note that, despite the fact that they are not equivalent from a structural point of view, the four nitroxide radicals have been considered as magnetically equivalent in eq 1. This simplifies considerably the model and avoids overparametrization. The best fit was obtained using the following parameters: $J_{Ni-rad} = -240$ K, $J_{rad-rad} = -14$ K, $g_{Ni} = 2.11$. To reproduce the decrease of the χT product, observed at temperatures below 50 K, it is necessary to introduce in the model an antiferromagnetic intermolecular interaction based on the mean-field approximation ($zj' = -2.3$ K). This has been performed by multiplying the calculated molar susceptibility (χ) (derived from the exchange Hamiltonian) by a factor equal to $(1 - zj'/Ng^2\mu_B^2)^{-1}$.

[Co(2,6-NITpy)$_2$](ClO$_4$)$_2$·0.5H$_2$O·CH$_3$OH (2). The value of $\chi T = 1.47$ emu K mol^{-1} at 300 K (Figure 4b) is very low compared to the calculated ("spin-only") value for one $S = 3/2$ and four $S = 1/2$ centers completely uncorrelated ($\chi T = 3.375$ emu K mol^{-1}). Morever, if the orbital degeneracy of the cobalt(II) ion is considered, a limiting value of $\chi T \approx 3.85$ emu K mol^{-1} should really be observed in the absence of interactions. Lowering the temperature produces a continuous linear decrease of the χT product until a value equal to 0.056 emu K mol^{-1} is reached at 1.83 K.

The magnetic data described here indicate a very strong antiferromagnetic coupling between the cobalt(II) center and the four nitroxide radicals. At very low temperatures, a diamagnetic ground state resulting from the coupling between the Co(II) Kramers doublet and the four peripheral $S = 1/2$ spins is observed. A quantitative treatment of the susceptibility data, including the orbital degeneracy of the cobalt(II) center, cannot be performed with our program. The calculation of the different coupling parameters has thus been omitted.

[Zn(2,6-NITpy)$_2$](ClO$_4$)$_2$·2.5CH$_3$CN (3). The value of the χT product (Figure 5a) at 300 K (1.36 emu K mol^{-1}) is somewhat smaller than the corresponding value for four uncorrelated nitroxide radicals (1.50 emu K mol^{-1}). As the sample is cooled, χT decreases continuously and eventually drops to zero at the lowest temperatures. The temperature dependence of the molar magnetic susceptibility (Figure 5b) shows a maximum at $T = 42$ K, where $\chi = 0.0151$ emu mol^{-1}.

These results give evidence for a diamagnetic ground state that arises from spin pairing of adjacent nitroxide radicals *within the same cationic complex*. An intermolecular interaction between nitroxide radicals belonging to neighboring molecules would be of the same order of magnitude or even weaker that the one observed in the nickel(II) compound **1**, which has a similar but more compact structure. Such a value cannot explain the presence of a maximum in the χ versus T curve at relatively high temperatures. A nonmagnetic ground state would also result from two different radical−radical interactions, one being ferromagnetic and the other one antiferromagnetic. Note, however, that the dihedral angles between proximate radicals are very similar (mean value: 81(4)°) and deviate considerably from 90°. Thus, a very good agreement between experimental and calculated values has been obtained by considering only one nearest-neighbor antiferromagnetic interaction ($J_{rad-rad}$) between radicals coordinated to the same metal center. After diagonalization of the corresponding Hamiltonian (second term of eq 1), the fitting procedure affords a value of the radical−radical exchange coupling parameter, $J_{rad-rad} = -27.7$ K. This value has been taken as an estimate of $J_{rad-rad}$ in the other complexes herein studied.

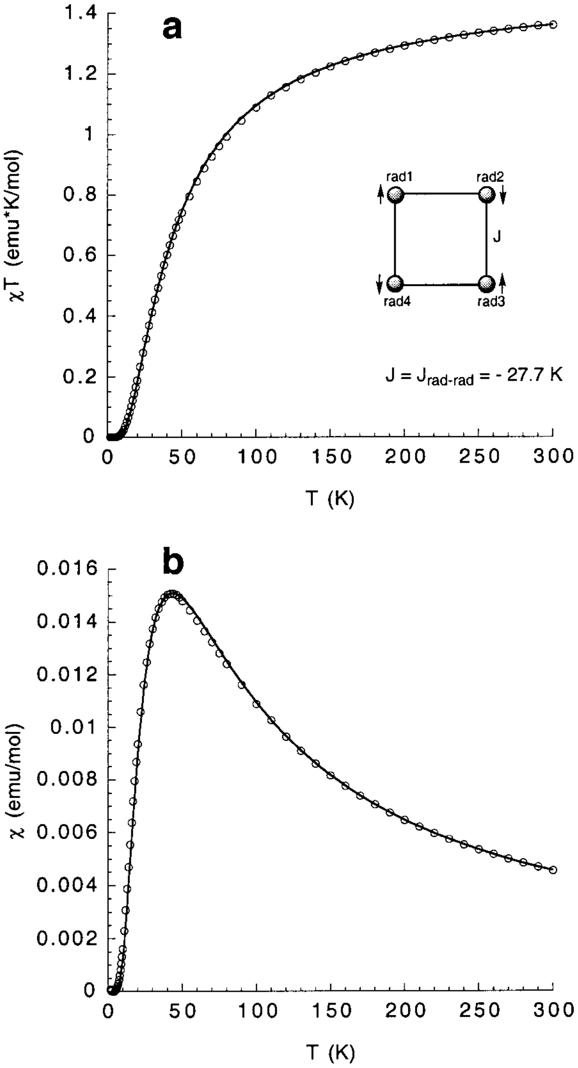

Figure 5. Temperature dependence of χT (a) and χ (b) for **3**. The solid lines represent the best-fit calculated data. Inset: Exchange interaction patterns and values of the calculated parameters.

[Mn(2,6-NITpy)$_2$](ClO$_4$)$_2$·1.5CH$_2$Cl$_2$·0.5C$_5$H$_{10}$O$_2$ (4). The χT product at room temperature (1.48 emu K mol^{-1}) is well below (Figure 6a) the calculated value for an uncorrelated system containing a manganese(II) cation ($S = 5/2$) and four $S = 1/2$ spins ($\chi T = 5.875$ emu K mol^{-1}). Cooling the sample induces a monotonic decrease of χT until a plateau is reached in the 60−25 K region, where the average value of χT is 0.37 emu K mol^{-1}. At temperatures lower than 20 K, χT decreases abruptly and tends to zero ($\chi T = 0.075$ emu K mol^{-1} at 1.83 K).

The nearly constant value of $\chi T \approx 0.37$ emu K mol^{-1} observed at low temperatures points to the existence of a $S = 1/2$ ground state that results from antiferromagnetic coupling

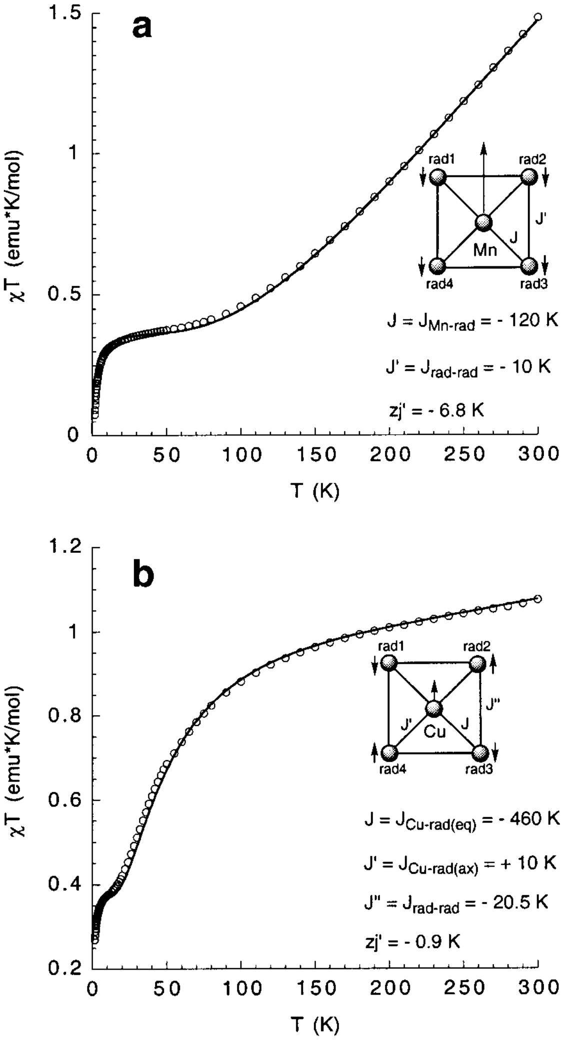

Figure 6. Temperature dependence of the product of the molar magnetic susceptibility with temperature (χT) for **4** (a) and **5** (b). The solid lines represent the best-fit calculated data. Insets: Exchange interaction patterns and values of the calculated parameters.

between the manganese(II) ion and the four radicals located in its coordination sphere. A coupling scheme similar to that used in the modeling of the magnetic properties of compound **1** has been employed (see inset Figure 6a). The corresponding isotropic spin Hamiltonian is thus obtained from eq 1 by considering now S_{Mn} instead of S_{Ni}. An intermolecular interaction ($zj' = -6.8$ K) has been taken into account in order to explain the decrease of the χT product observed below 20 K. The calculated values of the remaining parameters were found to be $g = 2.0$, $J_{Mn-rad} = -120$ K, $J_{rad-rad} = -10$ K.

[Cu(2,6-NITpy)$_2$](ClO$_4$)$_2$·CH$_3$CN (5). At room temperature, χT is equal to 1.08 emu K mol^{-1}, a value considerably lower (Figure 6b) than that expected (1.875 emu K mol^{-1}) for five noninteracting $S = 1/2$ spins. Lowering the temperature produces a continuous decrease of the χT product until a critical point is observed around 12 K, where $\chi T = 0.38$ emu K mol^{-1}. Cooling the sample further produces a sharper decrease, and χT equals 0.27 emu K mol^{-1} at the lowest temperature of the measurement (1.80 K).

Again, antiferromagnetic interactions seem to be dominant in this complex. The susceptibility data, however, suggest a $S = 1/2$ ground state, which cannot result from the interaction scheme that has been proposed for complexes **1**−**4**. A doublet ground state can appear if the dominant antiferromagnetic interactions are those between adjacent radicals. In this case, the doublet populated at low temperatures corresponds to the $S = 1/2$ spin of the copper(II) ion. Another possibility is to consider that only two nitroxide radicals are antiferromagnetically coupled to the metal center, the other two being ferromagnetically coupled.

The first hypothesis assumes that radical−radical interactions prevail over the copper−radical coupling. This is unlikely to be the case. Copper−nitroxide interactions are on the order of, at least, several tenths of cm^{-1}. Taking this fact into account, the data can only be roughly reproduced with a radical−radical coupling constant of some hundreds of wavenumbers, and this is a very high value, when compared to compounds **1**−**4**.

The second assumption offers a good agreement between model and experimental data. Two different copper−radical coupling constants have been introduced in the isotropic Hamiltonian:

$$H = -2J_{Cu-rad(eq)}(S_{Cu}S_{rad1} + S_{Cu}S_{rad2}) - 2J_{Cu-rad(ax)}(S_{Cu}S_{rad2} + S_{Cu}S_{rad4}) - 2J_{rad-rad}(S_{rad1}S_{rad2} + S_{rad2}S_{rad3} + S_{rad3}S_{rad4} + S_{rad4}S_{rad1}) \quad (2)$$

The fitting procedure afforded the following values for the different parameters: $g = 2.0$, $J_{Cu-rad(eq)} = -460$ K, $J_{Cu-rad(ax)} = +10$ K, $J_{rad-rad} = -20.5$ K, and a weak intermolecular interaction $zj' = -0.9$ K. Labels *eq* and *ax* refer, respectively, to equatorially and axially bound radicals (see Discussion section). Note the strong value of the antiferromagnetic copper−nitroxide interaction. At room temperature, two radicals are completely coupled to the copper(II) ion, leading to a $S = 1/2$ state. The other two radicals are not interacting at this temperature, and a limiting value close to that corresponding to three uncorrelated $S = 1/2$ spins ($\chi T = 1.125$ emu K mol^{-1}) should be observed, as indeed is the case.

Discussion

Whereas in most coordination compounds magnetic coupling takes place via a *superexchange* mechanism, the study of metal−nitroxide complexes (in which the two interacting spin carriers are directly bound) provides typical examples of *direct exchange*. In these systems, the magnetic orbitals are simply the half-occupied orbitals of each magnetic center. The magnetic orbital of the nitronyl nitroxide radical is a π^* orbital with its axis lying perpendicular to the O−N−C−N−O plane.[31] The magnetic orbitals for the different metal ions are given by simple ligand-field considerations. Following the Kahn−Briat rules,[32] the extent of overlap between metal and radical magnetic orbitals is responsible for the appearance of antiferromagnetic interactions, whereas orthogonality (or symmetry-forbidden overlap) of the same orbitals induces ferromagnetic contributions. With these ideas in mind, it is possible to correlate the metal−radical coupling to the crystal structures of the complexes.[33]

In our series of complexes, apart from these bonding interactions, it is also necessary to consider exchange coupling between radicals located in the same metal coordination sphere. In fact, contacts between nitroxide groups as short as 2.7 Å are observed.

---

(31) Zheludev, A.; Barone, V.; Bonnet, M.; Delley, B.; Grand, A.; Ressouche, E.; Rey, P.; Subra, R.; Schweizer, J. *J. Am. Chem. Soc.* **1994**, *116*, 2019−2027.

(32) Kahn, O.; Briat, B. *J. Chem. Soc., Faraday Trans. 2* **1976**, *72*, 268.

(33) Caneschi, A.; Gatteschi, D.; Grand, A.; Laugier, J.; Rey, P.; Pardi, L. *Inorg. Chem.* **1988**, *27*, 1031−1035.

The use of zinc(II) complexes as diamagnetic probes is a valuable tool to explore the origin and magnitude of these interradical interactions. A fairly strong ($J_{rad-rad} = -27.7$ K) antiferromagnetic coupling between adjacent radicals has been calculated from the susceptibility measurements of complex **3**. This interaction can be transmitted by different pathways, namely, (i) through bonds, within the same biradical chelate, (ii) through the diamagnetic metal center, and (iii) through space. Case (i) can be easily discarded by examining the previous reports on the 2,6-NITpy ligand. This compound has been isolated in two crystalline forms: an α-phase showing global antiferromagnetic behavior[34,35] and a *β*-phase[36] exhibiting short-range ferromagnetic interactions. A close inspection reveals that, whereas the conformation of the ligand is nearly the same in both phases, strong differences exist in their respective crystal packings. The magnetic interactions observed in pure 2,6-NITpy are thus intermolecular (propagated through space), and this is confirmed by susceptibility measurements made on solid solutions. Since the ligand conformation in complexes **1**−**5** does not differ significantly from the conformation observed in the α- and *β*-phases, propagation of radical−radical interactions within the same biradical chelate seems to be ineffective here.

Let us consider now case (ii). Magnetic coupling between radicals through a diamagnetic metal center seems to be the rule in some cases, for instance, in metal−semiquinonato complexes,[37,38] where appropriate metal and radical states are close in energy and mix considerably. In these compounds, charge-transfer states are low in energy and the unpaired electrons can be delocalized throughout the complex, thereby promoting magnetic interactions between proximate ligands. A mechanism involving excited charge-transfer states seems to be responsible for ferromagnetic coupling in a Cu(I)−imino nitroxide compound, in which two radicals bind to the metal center in an orthogonal arrangement.[39] However, charge-transfer states are very high in energy for Zn(II)−nitronyl nitroxide complexes, and this mechanism is unlikely to be responsible for the magnetic coupling in compound **3**.

The antiferromagnetic interactions between proximate radicals in compound **3** are then propagated through space. Thus, each radical interacts with the two radicals of the second ligand, and the use of a square-like interaction pattern (see Figure 5) is completely justified. Interaction through space has also been postulated in zinc complexes comprising three nitroxide ligands in the same coordination sphere.[22] In fact, in cases where the free radicals bind to the same zinc(II) center but remain relatively far apart from each other, only very small (intermolecular) interactions are observed.[16]

The correlation between the metal−radical coupling and the structural features of the remaining complexes is straightforward. For the Mn(II)−nitroxide complex (**4**), owing to the symmetry of the $^6A_1$ metal ground state, an antiferromagnetic interaction is expected.[40] The strong coupling observed ($J_{Mn-rad} = -120$ K ≈ -83 cm^{-1}) compares well with similar previously reported examples.[22]

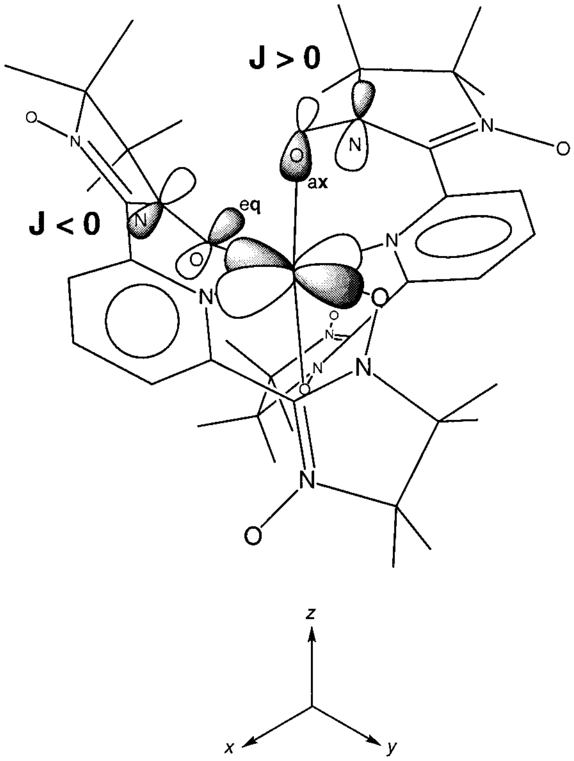

Figure 7. Representation of the overlap between the $d_{x^2-y^2}$ metal orbital and the π^* orbital of a nitronyl nitroxide located in axial and equatorial positions.

Nickel(II)−nitroxide complexes exhibit generally an antiferromagnetic behavior.[41] In some cases, however, a particular ligand design may induce ferromagnetic interactions.[16] In these examples the conjugated O−N−C−N−O group and the equatorial plane are coplanar. This brings the π^* radical orbital to be strictly orthogonal to the $d_{x^2-y^2}$ metal orbital, while its overlap with the d_{z^2} is symmetry-forbidden. This is far from being the case in complex **1**, where the angles between the equatorial plane and the different O−N−C−N−O groups lie in a range between 60° and 68° (see Table 2). This prominent deviation from coplanarity is responsible for the exceptionally strong nickel(II)−nitroxide antiferromagnetic coupling observed in this compound ($J_{Ni-rad} = -240$ K ≈ -167 cm^{-1}), one of the highest values ever reported in this kind of systems. Very strong antiferromagnetic interactions are also observed in the isostructural cobalt(II) complex, although a quantitative description of the magnetic behavior has not been performed.

Another interesting compound among the series is the copper(II) complex (**5**). A distinctive feature of compound **5** is that two nitroxide groups bind in axial positions. It is generally accepted that the interaction between a copper(II) center and an axially bound nitroxide radical is ferromagnetic because, in this geometry, the π^* radical orbital is strictly orthogonal (see Figure 7) to the $d_{x^2-y^2}$ metal orbital.[33] Thus, the positive value of the copper(II)−nitroxide coupling constant ($J_{Cu-rad(ax)} = +10$ K) has been ascribed to the interaction between the copper(II) ion and the radicals located in axial positions. The relatively low value observed arises from the fact that the Cu−O(ax) distances are fairly long (Jahn−Teller effect). The equatorially

---

(34) Sugano, T.; Tamura, M.; Kinoshita, M. *Synth. Met.* **1993**, *55*−*57*, 3305.

(35) Oshio, H.; Ohto, A.; Fujisawa, J.; Watanabe, T.; Ito, T.; Isobe, K. *Chem. Lett.* **1994**, 2353−2356.

(36) Drillon, M.; Hornick, C.; Laget, V.; Rabu, P.; Romero, F. M.; Rouba, S.; Ulrich, G.; Ziessel, R. *Mol. Cryst. Liq. Cryst.* **1995**, *273*, 125−140.

(37) Lange, C. W.; Conklin, B. J.; Pierpont, C. G. *Inorg. Chem.* **1994**, *33*, 1276−1283.

(38) Bruni, S.; Caneschi, A.; Cariati, F.; Delfs, C.; Dei, A.; Gatteschi, D. *J. Am. Chem. Soc.* **1994**, *116*, 1388−1394.

(39) Oshio, H.; Watanabe, T.; Ohto, A.; Ito, T.; Ikoma, T.; Tero-Kubota, S. *Inorg. Chem.* **1997**, *36*, 3014−3021.

(40) Caneschi, A.; Gatteschi, D.; Laugier, J.; Rey, P.; Zanchini, C. *Inorg. Chem.* **1988**, *27*, 2027−2032.

(41) Caneschi, A.; Gatteschi, D.; Renard, J. P.; Rey, P.; Sessoli, R. *Inorg. Chem.* **1989**, *28*, 2940−2944.

(42) Spek, A. L. *PLATON 99*, *Multipurpose Crystallographic Tool*; Utrecht University: The Netherlands, 1999.

bound nitronyl nitroxide radicals couple antiferromagnetically to the copper(II) ion. A very large value of the exchange coupling parameter ($J_{Cu-rad(eq)} = -460$ K) has been observed. The dihedral angles between the equatorial plane and the O−N−C−N−O groups deviate considerably from 0° (see Table 2), and the same arguments that were developped in the discussion of the Ni(II) complex apply also here. The strong value of $J_{Cu-rad(eq)}$ correlates well with the very short Cu−O(eq) distances (1.955 Å) observed.

Any attempt to correlate the intermolecular magnetic interactions observed at low temperatures to particular structural features is hindered by the presence of four free nitroxide groups per cationic complex. Only in the case of the manganese(II) complex (**4**) it is possible to ascribe the strong antiferromagnetic intermolecular interaction ($zj' = -6.8$ K) to the existence of dimers related by a center of symmetry. The crystal structure of the copper(II) complex shows that the uncoordinated nitroxide groups are relatively well separated. Accordingly, a very weak intermolecular interaction ($zj' = -0.9$ K) has been calculated.

Conclusion

The synthesis, characterization, and magnetic properties of a new series of metal complexes based on a terdentate nitronyl nitroxide biradical (2,6-NITpy) have been described. It has been shown that it is possible to increase the number of free radicals in the metal coordination sphere by an appropriate ligand design. In these cases, however, interactions between adjacent radicals in the same coordination sphere have to be considered. The coordination mode of 2,6-NITpy favors a strong overlap between metal and radical magnetic orbitals. Exceptionally large Ni(II)−nitroxide and Cu(II)−nitroxide antiferromagnetic interactions have been observed. The strength of these interactions has been correlated to suitable structural features.

Axially and equatorially bound nitroxide functions alternate in the same coordination sphere of the copper(II) complex (**5**). The radicals located in axial position couple ferromagnetically to the copper center, whereas the coupling between the metal ion and the radicals that bind in the equatorial plane is antiferromagnetic. We are not aware of other previously reported example showing this behavior. Complex **5** could be interesting in the context of pseudo spin transitions. Indeed, we are now exploring the dynamic behavior of this compound in order to gain insight into the possible equilibrium between axially and equatorially ligated radicals.

Acknowledgment. The authors are pleased to thank Dr. J. M. Clemente-Juan for providing them access to ISOMAG, a program for the calculation of magnetic susceptibility. Dr. F. M. Romero thanks the Spanish M.E.C. (Ministerio de Educación y Cultura) for a research contract (Contrato de Reincorporación). This work was partly funded by the TMR Research Network ERBFMRXCT 980181 of the European Union, entitled “Molecular Magnetism: From Materials towards Devices”, and by the Swiss National Science Foundation through Project No. 21-52699.97.

Supporting Information Available: Crystallographic data for compounds **1**−**5** have been deposited in the CIF format. This material is available free of charge via the Internet at http://pubs.acs.org.

IC991236A